Research Article

Görkem Ozankaya, Mohammed Asmael, Mohamad Alhijazi, Babak Safaei*, Mohamed Yasin Alibar, Samaneh Arman, Kamila Kotrasova*, Vincent Kvocak, Michala Weissova, Qasim Zeeshan, and David Hui

Prediction of lap shear strength of GNP and TiO_2/epoxy nanocomposite adhesives

https://doi.org/10.1515/ntrev-2023-0134
received January 11, 2023; accepted September 23, 2023

Abstract: In this study, graphene nanoplatelets (GNPs) and titanium dioxide nanofillers were added to epoxy resin P-5005 at five different weight percentages (wt%), *viz*., 1, 5, 10, 15, and 20 wt%. The tensile properties of the nanocomposites were experimentally tested following ASTM D638-14. Then, the above-mentioned nanocomposites were applied as adhesives for an overlap joint of two A5055 aluminum sheets. The apparent shear strength behavior of joints was tested following ASTM D1002-01. Moreover, experimentally obtained results were applied to train and test machine learning and deep learning models, *i.e.*, adaptive neuro-fuzzy inference system, support vector machine, multiple linear regression, and artificial neural network (ANN). The peak tensile strength (TS) and joint failure load (FL) values were observed in epoxy/GNP samples. The ANN model exhibited the least error in predicting the TS and FL of the considered nanocomposites. The epoxy/GNP nanocomposites exhibited the highest TS of 28.49 MPa at 1 wt%, and the peak overlap joints exhibited an FL of 3.69 kN at 15 wt%.

Keywords: graphene nanoplatelets, titanium dioxide, mechanical characteristics, machine learning

*** Corresponding author: Babak Safaei,** Department of Mechanical Engineering, Eastern Mediterranean University, Famagusta, North Cyprus via Mersin 10, Turkey, e-mail: babak.safaei@emu.edu.tr
*** Corresponding author: Kamila Kotrasova,** Institute of Structural Engineering and Transportation Structures, Faculty of Civil Engineering, Technical University of Kosice, Vysokoskolska 4, 042 00 Kosice, Slovakia, e-mail: kamila.kotrasova@tuke.sk
Görkem Ozankaya, Mohammed Asmael, Mohamed Yasin Alibar, Qasim Zeeshan: Department of Mechanical Engineering, Eastern Mediterranean University, Famagusta, North Cyprus via Mersin 10, Turkey
Mohamad Alhijazi: School of Engineering, Lebanese International University LIU, Bekaa, Lebanon
Samaneh Arman: School of Science and Technology, The University of Georgia, Tbilisi 0171, Georgia
Vincent Kvocak, Michala Weissova: Institute of Structural Engineering and Transportation Structures, Faculty of Civil Engineering, Technical University of Kosice, Vysokoskolska 4, 042 00 Kosice, Slovakia
David Hui: Department of Mechanical Engineering, University of New Orleans, New Orleans, LA 70148, United States of America

1 Introduction

Epoxy resin is one of the most vital structural adhesives, widely popular in aerospace, automotive, electronics, civil, and packaging industries. Recently, the adhesive industry has changed significantly by including new formulations, raw materials, substrates, operation conditions, applications, and curing processes [1]. Therefore, properties such as resistance to failure at vibration and fatigue loading, resistance to thermal cycling and high service temperatures, and optimum curing conditions have to be considered in epoxy adhesives. Numerous studies aimed to develop multifunctional epoxy adhesives by mixing epoxy with a second material as a filler, such as carbon nanotubes (CNTs), graphene, Al_2O_3, $CaCO_3$, SiO_2, ZrO_2, titanium dioxide (TiO_2) and so on. In recent years, the size of fillers has shifted from micro- to nano-scale, resulting in much superior multifunctional characteristics in nanocomposite adhesives compared to neat adhesives and their composites having conventional micro-particles [2,3]. The addition of nanoparticles to epoxy adhesive joints improves their mechanical properties, joints' failure load (FL), thermal stability, and electrical conductivity [4–7]. However, it varies based on several parameters, such as particle characteristics, functional groups on the nanoparticle surface, size distribution, size, content, and shape, defining its compatibility with the epoxy matrix [8–12].

Graphene is a carbon allotrope that consists of a one-atom layer and its lattice nanostructure is arranged in a 2D honeycomb structure. Since 2004, it has been considered one of the most stiff and strong materials. The Young's modulus and tensile strength (TS) of graphene are around 1 TPa and 130 GPa, respectively [13]; moreover, the thermal conductivity is around 5,000 W/mK [14]. Multilayered

graphene, also known as graphene nanoplatelets (GNPs), has become a very desirable polymer matrix filler with a great price-to-performance ratio and is utilized in diverse fields, *i.e.*, energy, defense, electronics, transport, medicine, *etc.* TiO_2, which is also known as titanium, is a natural mineral available in various crystalline structures, and its applications include the textile industry, food products, coatings, plastics, pharmaceuticals, and so on.

Multiple research studies have investigated the mechanical, thermal, and electrical characteristics of epoxy adhesives reinforced with GNP and metal-based TiO_2. Singh *et al.* [15] studied the effect of GNP and multi-walled carbon nanotubes (MWCNTs) on the mechanical characteristics of epoxy-based nanocomposites, and the results showed that the epoxy/GNP composite provided greater tensile and compressive strengths compared to MWCNT/epoxy composites, while the latter exhibited a greater toughness compared to epoxy/GNP. Hence, graphene possesses an outstanding specific surface area, in addition to significant mechanical and electrical properties, which makes graphene the greatest compared to other carbon allotropes for developing multifunctional and structural-reinforced composites [16,17]. Moreover, the dispersion of graphene in the composites and the surface friction force of graphene are the two main properties that have an impact on the ability of graphene to improve damping [18–20].

Mustafa *et al.* [21] have studied the influence of MWCNTs on mechanical characteristics and thermal stability of hybrid nanocomposites. The hybrid polymer structure was made from epoxy resin mixed with different weight percentages of zirconium dioxide (ZrO_2) and yttrium oxide (Y_2O_3). The structure was further strengthened with 0.1 wt% MWCNT through a hand lay-up casting process. It was reported that the TS and Young's modulus were improved by 24 and 37% in comparison with pure epoxy resin. Kumar *et al.* [22] investigated the tensile and dynamic mechanical properties of epoxy/MWCNT/TiO_2 hybrid nanocomposites at 0.25, 0.5, 0.75, 1, and 1.5 wt%. The results revealed that the TS of epoxy was increased by 24% by the addition of 1 wt% MWCNTs. Modeling and simulation as well as artificial intelligence have emerged in a wider spectrum for diverse science and engineering applications [23–25]. Even though experimental testing is drastically crucial for the development of new material, machine learning reduces the computational time and cost, since the needed platforms to run machine learning algorithms mainly have free access and can be found easily [26–28]. Artificial intelligence was recently implemented by numerous studies to analyze the characteristics of composite materials, natural fiber composites, and nanocomposites [29–33]. Pati [34] utilized artificial neural networks (ANNs) to predict the wear properties of glass/epoxy composites, and the input data included the RBD content, erodent size, erodent temperature, impact velocity, and impingement angle. Antil *et al.* [35] applied the response surface metamodel and ANN to evaluate the erosion characteristics of S glass composites, and the input parameters consisted of the impingement angle, nozzle diameter, and slurry pressure. Jayaganthan *et al.* [36] classified the conductivity of epoxy reinforced with 66 wt% silica fillers, 0.7 wt % ion trapping particles and coated with four different coal types by implementing a support vector machine (SVM), logistic regression model, *K*-nearest neighbors, and a multi-layer perceptron approach in their LIBS spectral data. Rahman *et al.* [37] applied a convolutional neural network for the analysis of the pull-out force of epoxy/CNT nanocomposites.

The goal of the current research was to study the characteristics of epoxy reinforced with GNP and TiO_2 nanoparticles for aluminum single-lap joint application by testing the tensile properties of the considered nanocomposites, examining nanocomposite joints' FL, and developing an SVM, multiple linear regression (MLR)-based metamodel, adaptive neuro-fuzzy inference system (ANFIS), and ANNs. The effect of increasing filler weight percentages of 1, 5, 10, 15, and 20 wt% was examined.

2 Methodology

TiO_2 and GNP nano-particles were added into an epoxy matrix with five different percentages, *i.e.* 1, 5, 10, 15, and 20 wt%. First, the tensile behaviors of these nanocomposites were evaluated following the ASTM D638-14 tensile testing standard, followed by scanning electron microscopy for testing the fracture surface morphology. Moreover, the aforementioned nanocomposites were applied as an overlap adhesive between two aluminum plates. The apparent shear strength properties of the adhesives were tested following ASTM D1002-01. The experimental results were utilized to train and test machine learning and deep learning models, *i.e.*, ANFIS, SVM, MLR, and ANN to evaluate the ability of the aforementioned to predict the mechanical properties of nanocomposites.

2.1 Experiment

Epoxy resin P-5005 by Polymex was utilized in this study as a matrix for the nanocomposite adhesive. The resin-to-hardener mixing ratio (2:1) and matrix-to-filler

compositions were prepared using a high-precision electronic balance. Thus, in order to achieve a homogeneous nanocomposite, the nanocomposites were prepared *via* the following steps: a specific amount of epoxy was added into the mixing container, then nanoparticles were added upon a desired weight percentage, and the mixture was stirred with a plastic spoon for 25 min. To ensure that the nanoparticles in the epoxy were evenly distributed, the mixture was left at room temperature for an extra 2 h. After the addition of the curing agent, the mixture was mixed for 3 min, and then poured into a mold to develop tensile test specimens and to prepare lap-shear test samples The A5055 aluminum sheets (1 mm thick) were considered as an adherent material. Moreover, the sheets' surfaces were wiped and treated aiming to enhance the bonding between the nanocomposite material and the aluminum sheets. GNPs and TiO_2 were supplied from Nanografi. GNPs had a purity of 99.9%, 5 nm thickness, 30 µm diameter, gray in color, a conductivity between 1,100 and 1,600 s/m, and a specific surface area of 170 m^2/g. TiO_2 nanoparticles were of 20 nm size, 99.9% purity, 4.26 g/cm^3 density, white in color, and 79.87 g/mol molecular weight.

2.1.1 Tensile test

The TS values of GNP and TiO_2-reinforced epoxy nanocomposites were tested following the ASTM standard D638-14. Dog bone-shaped samples were prepared with 200 mm length, 57 mm width, 3.2 mm thickness, and a gauge length of 50 mm. First, the epoxy resin and its hardener were mixed in a 2:1 ratio and then the nanoparticles were added and stirred until the mixture became homogeneous. A layer of releasing agent was sprayed into the wooden mold before pouring the mixture. Then, the samples were cured at room temperature for 12 h. The test was conducted on an INSTRAM 338571 tensile machine with a testing speed of 5 mm/min.

2.1.2 Lap joint

A5055 aluminum was selected as a substrate material. Single lap joint specimens were prepared by first slightly roughening the overlap area using an emery cloth to strengthen the bonding between the adhesive and substrates, followed by immersing the latter in a detergent to prevent any unwanted dirt, grease, or oil. Then, the samples were removed from the solution, washed with deionized water, and dried using a tissue. An epoxy/nanoparticles mixture was then spread for a 25 mm × 25 mm overlap area, keeping a grip length of 200 mm (Figure 1). Thus, the thickness of the cured adhesive was around 0.5 mm. In order to ensure the results' accuracy and avoid undesired errors, three replicates were prepared for each nanocomposite's composition, *i.e.*, 1, 5, 10, 15, and 20 wt%. An INSTRAM 338571 tensile machine (10 kN) was utilized for conducting the single lap joint test at a testing rate of 1 mm/min.

2.2 Machine learning and deep learning predictions

Machine learning is derived from artificial intelligence, which is a method that trains the computer to perform tasks that are usually specific for humans and acquired through experience. Increasing the amount of learning samples usually enhances the precision of the algorithm. Moreover, the implementation of deep learning in research attained wide popularity since 2006, as it was applied to

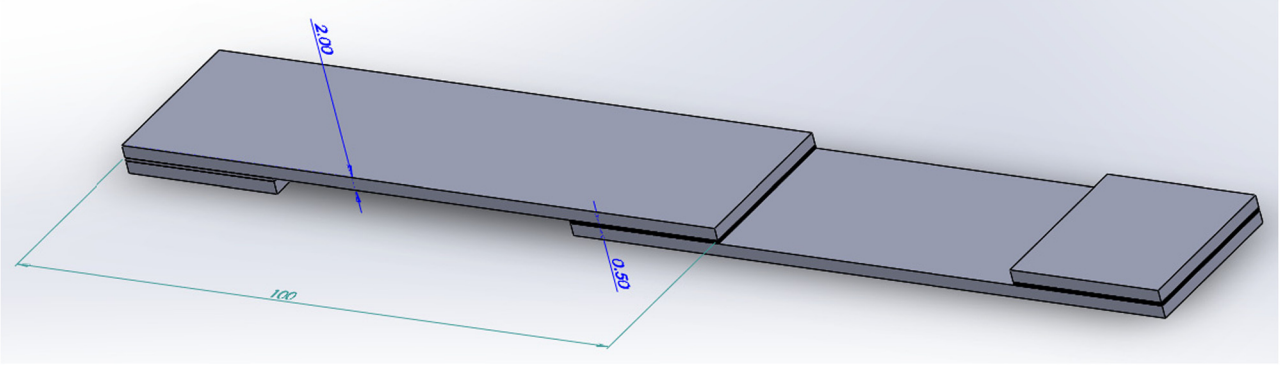

Figure 1: The geometry of adhesively bonded aluminum joints.

object recognition, machine translations, speech recognition, and image segmentation. Basically, due to their neural network structures, most deep learning methods could be considered deep neural networks. Although there are supervised and unsupervised machine learning algorithms, the former is more suitable for manufacturing implementations due to the labeled data it provides:

$$\text{Prediction error } \% = \frac{|\text{Expt. Value} - \text{Pred. Value}|}{\text{Expt. Value}} \times 100. \quad (1)$$

An easy approach for evaluating the training model precision is called prediction error, where the aforementioned is validated using novel input data, which were not considered in the testing stage, which thereby contributes to defining the error percentage. Hence, root mean square error (RMSE) is a prevalent method used to define a model's error:

$$\text{RMSE} = \sqrt{\frac{1}{N}\sum_{i-1}^{N}(p_i - q_i)^2}, \quad (2)$$

where N is the whole training data, p_i is the predicted deliberate information, and q_i is the real value.

In this study, ANFIS, SVM, ANNs, and the response surface metamodel were applied to evaluate and define the most suitable approach for the prediction of the lap shear strength and TS for input parameters not considered in the experiment, as well as to determine the design space based on the considered parameters. The proposed model employs nanoparticle types and weight percentages as input. The tensile test and shear lap experimentally obtained results were considered for training, validation, and testing. The precision of the prediction models was assessed by the mean value of absolute percentage error.

3 Results and discussion

The tensile and shear characteristics obtained from experimental and machine learning of TiO_2 and GNP-reinforced epoxy are presented in this section.

3.1 Tensile test

In this section, tensile test results are presented, which mainly highlight the TS values of epoxy/GNP and epoxy/TiO_2 nanocomposites for five different compositions. Figure 2 illustrates the impact of increasing TiO_2 and GNP nanoparticles from 1 to 20 wt% on the TS of the end nanocomposites.

As exhibited in Figure 2, increasing the TiO_2 content increased the TS from 17.96 to 25.23 MPa at 10 wt%, which was the highest TS observed in TiO_2-reinforced nanocomposites. Meanwhile, the addition of GNP in the epoxy matrix reached the highest TS value of 28.49 MPa at 1 wt% followed by a gradual decrease to reach 20.22 MPa at 20 wt%. Close TS values of 25.23 and 25.07 MPa were observed in both nanocomposites at 10 wt%, respectively. Thereby, GNP and TiO_2 nanocomposites followed a descending trend to reach 20.22 and 20.37 MPa at 20 wt%. The highest TS value recorded in this study was observed in GNP-reinforced epoxy at 1 wt%, which was quite similar to the results obtained by Nitesh *et al.*

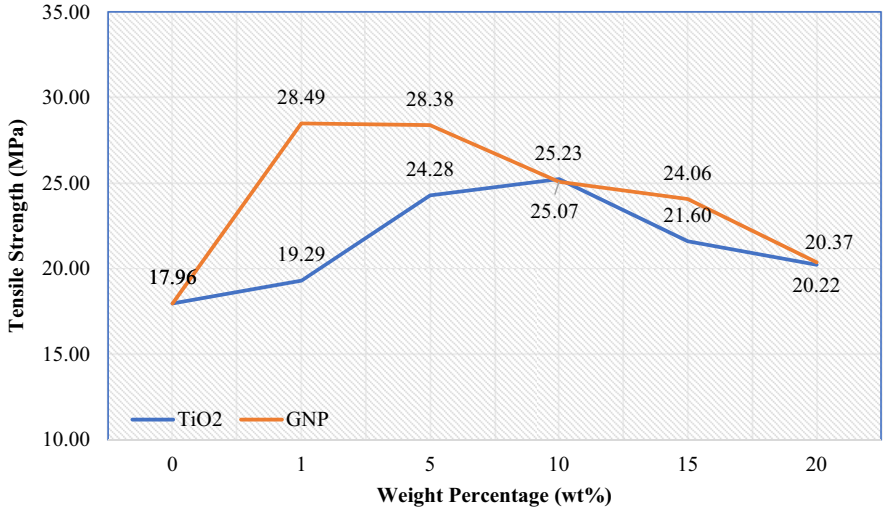

Figure 2: TS of epoxy/TiO_2 and epoxy/GNP for 5 wt%.

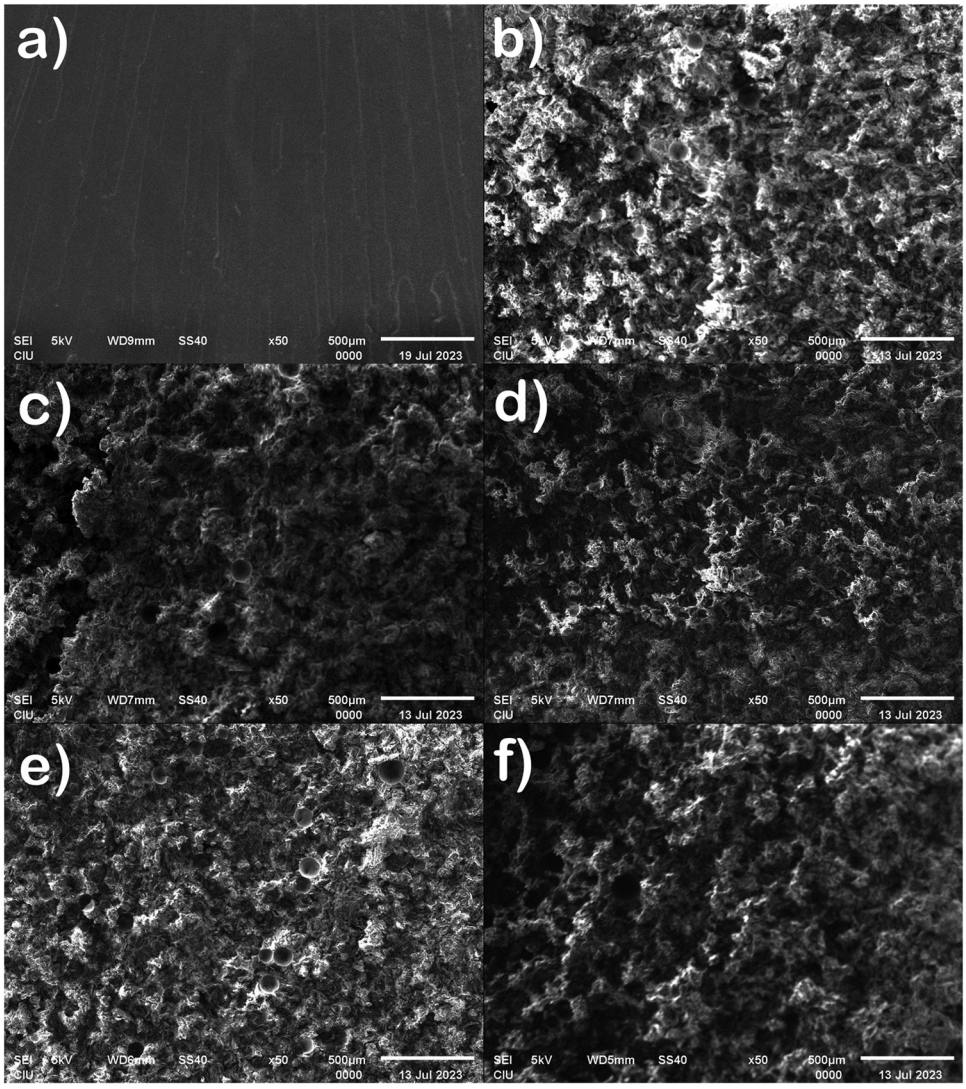

Figure 3: Fracture surface of nanocomposite epoxy with different GNP contents: (a) 0 wt%, (b) 1 wt%, (c) 5 wt%, (d) 10 wt%, (e) 15 wt%, and (f) 20 wt%.

[38], where a 1 wt% nanoparticle concentration exhibited the highest tensile behavior, which was ~60% higher than the corresponding values obtained for neat epoxy. The decrease in the TS when the filler content is further increased above the optimal concentration is caused by the agglomeration of the nanofillers, which thereby leads to weaker interface bonding between the matrix and the fillers. Figure 3 illustrates SEM micrographs of the epoxy fracture surface at 1, 20, 5, 10, and 15 wt% GNP.

Larger agglomerates were observed when the GNP content exceeded 1%. The 20% GNP ductile epoxy specimen exhibited a significant agglomeration. Referring to the tensile test results, GNP/epoxy samples with GNP contents exceeding 5% exhibited decreased tensile modulus and TS, which could be due to the increase in the size and amount of agglomerates inside the nanocomposite [39]. The fracture surface of the nanocomposites became markedly rougher upon the increase of the nanofiller content. Figure 4 shows the SEM of epoxy/TiO_2 at five different weight percentages.

As clearly shown in Figure 4, TiO_2 exhibited a good dispersion along with a good interface compatibility with the epoxy matrix. Furthermore, scanning electron micrography of TiO_2 showed that the manufactured nanoparticles were made up of small, irregularly shaped, fine particles. Peeling away from the grain boundaries indicates brittle fracture, whereas the presence of many dimples indicates ductile fracture surface. Fracture in composites is caused by the initiation and expansion of dimples, fracture of the layers or reinforcing particles, and interface detachment. The SEM graphs show that these fracture surfaces exhibit ductile and cleavage modes of fracture.

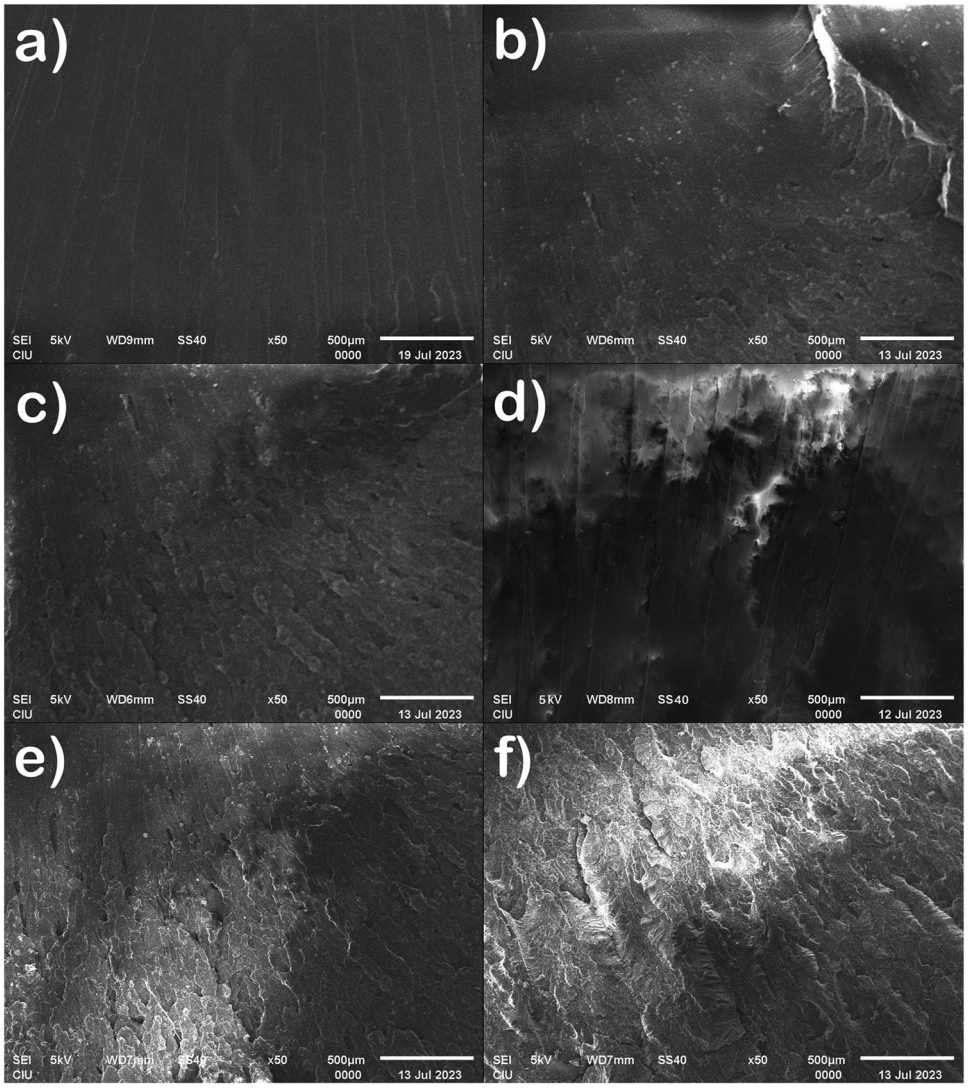

Figure 4: Fracture surface of the nanocomposite epoxy with different TiO_2 contents: (a) 0 wt%, (b) 1 wt%, (c) 5 wt%, (d) 10 wt%, (e) 15 wt%, and (f) 20 wt%.

3.2 Lap joint

The results of the apparent shear strength of aluminum specimens adhesively bonded with single lap joints are given in this section. GNP and TiO_2 nanocomposites at five different weight fractions were considered adhesives for aluminum overlap joints. Figure 5 shows FL *versus* displacement of epoxy/TiO_2 at 10 wt%.

As exhibited in Figure 5, ductile behavior was observed in epoxy/TiO_2 overlap joints; the force *vs* displacement behavior started with a linear elastic increase to reach a force of 1.108 kN at 0.075 mm. Then, the force increased gradually along with a notable increase in the displacement, where it attained a maximum value of 1.877 kN at 0.567 mm, right before its failure. Figure 6 displays the FL and displacement behavior of the epoxy/GNP lap joint at 15 wt%.

As shown in Figure 6, the force *vs* displacement of the epoxy/GNP nanocomposite at 15 wt% increased linearly to reach a value of 1.553 kN at 0.119 mm. Then, it followed an ascending trend to exhibit its peak force of 3.081 kN at 0.806 mm, which was straight before its ductile failure. Although the nanoparticles were evenly distributed throughout the hardened resin, the TS of the corresponding modified resin likewise significantly decreased [40]. The poorer interlocking system caused by inadequate dispersion within the composite matrix may be the cause of the decreased bond strength shown in specimens.

Figure 7 shows the comparison of the impact of increasing the filler content on the maximum FL.

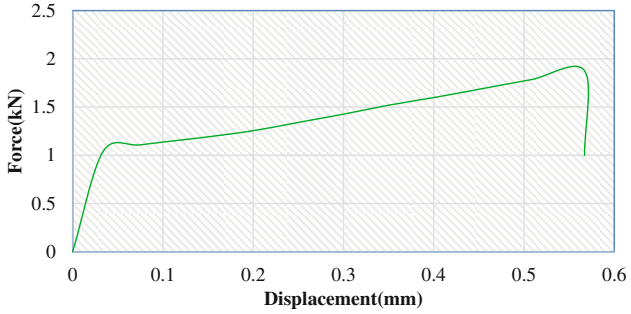

Figure 5: Force *vs* displacement of the epoxy/TiO_2 lap joint at 10 wt%.

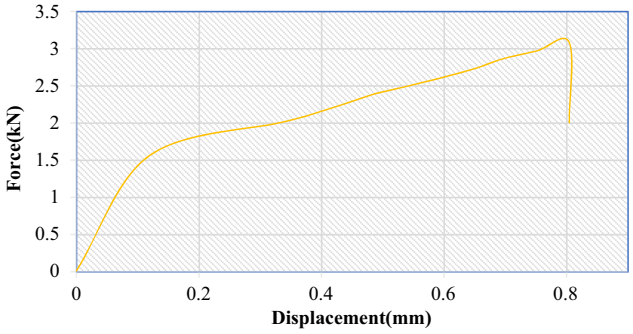

Figure 6: Force *vs* displacement of the epoxy/GNP lap joint at 15 wt%.

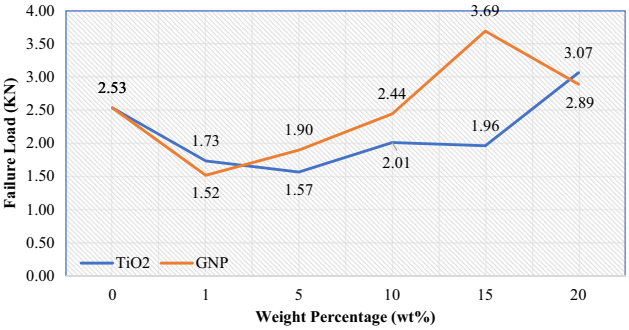

Figure 7: Joint FL of the epoxy/TiO_2 and epoxy/GNP for 5 wt%.

As displayed in Figure 7, the addition of 1 and 5 wt% TiO_2 nanoparticles decreased the joint shear strength compared to pure epoxy, revealing average FLs of 1.73 and 1.57 kN, respectively. Further increasing the weight percentage of TiO_2 led to an increase in the FL, which exhibited its peak value of 3.07 kN at 20 wt%. A common behavior was observed at 1 wt% GNP, where the joint FL decreased to 1.52 kN, which was around 60% lower than that of pure epoxy joints. Hence, increasing the GNP content contributed to increasing joint FL to reach its highest FL of 3.69 kN in the nanocomposite with 15 wt% GNP, followed by a decrease at 20 wt%. Throughout the considered compositions, 20 wt% revealed peak FL in TiO_2 nanocomposites, whereas 15 wt% was an optimum composition for epoxy/GNP nanocomposites, which was also considered as highest FL in this study (3.69 kN). The opposite FL behavior of both nanocomposites at 20 wt% can be explained by adapting some of the important properties of nanocomposites, *i.e.*, matrix to particle interface quality. In other words, if the interaction between the matrix and nanoparticles is weak, the particles are unable to withstand a part of the applied external loads to the nanocomposite, thereby the yielding of amorphous glassy polymers switches from cavitational to shear, leading to a brittle to ductile transition. It is worth mentioning that there are two types of damage, *i.e.*, adhesion and cohesion, and their occurrence is strongly correlated to the homogeneous dispersion of nanoparticles in the epoxy matrix. Therefore, the adhesion strength can be affected by physical and chemical reactions between the epoxy and nanofiller materials.

3.3 Machine learning and deep learning

MLR, ANNs, ANFIS, and SVM were applied in the current study to define the most suitable machine learning method to predict shear force and TS of nanocomposites, as well as specify design spaces of corresponding parameters. The results of the aforementioned machine learning tools in predicting TS and overlap joint FL of GNP and TiO_2 nanocomposites are listed in this section. A regression model was applied in this study by the curve fitting tool (Cftool) in MATLAB. Response surface models of GNP and TiO_2 nanocomposites were projected *via* cubic polynomial prediction functions. Moreover, output data were TS and FL, while input data were weight percentage and fiber type. Furthermore, the response surface metamodel creates a surface fit, which considers the whole design space, providing the ability to predict responses using input parameters not considered in the experiment. Figure 8a and b shows the developed response surfaces.

The Cftool in MATLAB was used to develop the RSM for the TS and overlap FL of TiO_2 and GNP nanocomposites. The RMSE, *R*-square adjusted, and sum of square error (SSE) were considered to evaluate goodness of fit. For proper surface fit, the values of SSE and RMSE should be as close as possible to 0. Meanwhile, the adjusted value of the *R*-square ranges from 0 and 1, and a good fit should be close to 1. Moreover, the function utilized to develop the response surface of the TS of nanocomposites is

$$f(x,y) = p00 + p10 \times x + p01 \times y + p11 \times x \times y + p02 \times y^2 + p12 \times x \times y^2 + p03 \times y^3,$$

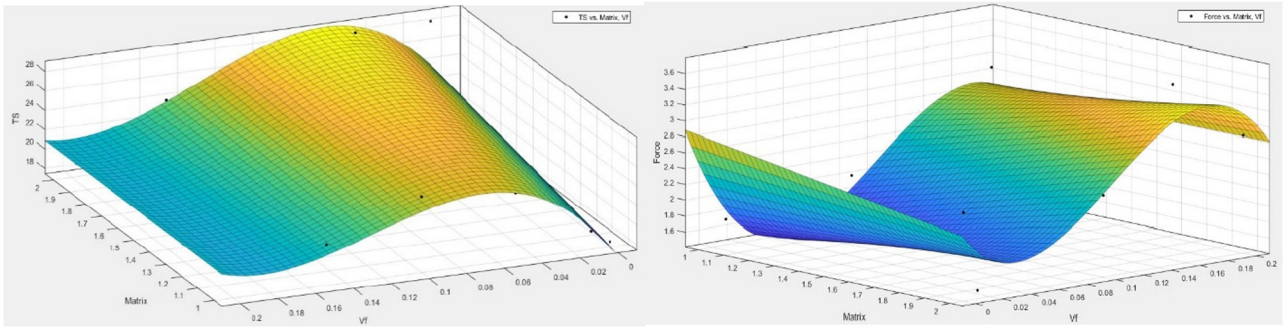

(a) (b)

Figure 8: Response surface fitting for the (a) TS and (b) joint FL.

where x is the nanoparticle type, y is the weight percent, and $p00$ =12.92, $p10$ = 4.418, $p01$ = 285.6, $p11$ = −22.2, $p02$ = −2,560, $p12$ = 7.554, and $p03$ = 6,555. The goodness of fit attained an RMSE of 2.896, adjusted R-square of 0.3909, R-square of 0.7232, and SSE of 41.94.

For the RSM model of overlap joints FL, the applied function was

$$f(x,y) = p00 + p10 \times x + p01 \times y + p11 \times x \times y + p02 \times y^2 + p12 \times x \times y^2 + p03 \times y^3,$$

where x is the nanoparticle types, y is the weight percent, and $p00$ = 2.708, $p10$ = −0.3022, $p01$ = −62.74, $p11$ = 22.09, $p02$ = 555, $p12$ = −97.93, and $p03$ = −1,213. In addition, SSE = 1.168, RMSE = 0.4832, adjusted R-square = 0.4671, and R-square = 0.7578.

All components of the prediction model in this study were trained using the Levenberg–Marquardt algorithm, which exhibited a stable and swift convergence. Figure 9 illustrates the ANN model design: it consisted of 2 inputs, 10 hidden layers, and a single output.

A neural network fitting tool in MATLAB was utilized for the generation of the ANN models. Nanoparticle types and weight percentages were considered as input data, whereas the TS and FL were the model outputs. Experimental results of the tensile test and overlap shear test were considered to generate two corresponding models, and 70% of the data were utilized for training, 15% for validation, and 15% for testing. Figure 10 shows the schemes of TS regressions for TiO_2 and GNP nanocomposites for five different weight percentages, *i.e.*, 1, 5, 10, 15, and 20 wt%. This graph provides a correlation between experimental data (target) and ANN output data.

As shown in Figure 10, the dotted line denotes the best achievable correlation, while the solid line represents the correlation between output and target values. The overall regression coefficient of the TS ANN model was 0.93712 and that of the FL ANN model was 0.92341, which can be considered satisfactory as the values are close to 1. The MATLAB regression learner tool was used to generate the SVM model, and input parameters included two nanoparticle types and five weight percentages. Testing and training output datasets created by the FL SVM model are shown in Figure 11: yellow dots illustrate predicted data, while blue dots are the true data.

Furthermore, SVM models were trained using tensile and FL experimental results, Gaussian was considered as the kernel function, and fine Gaussian SVM was the selected preset. However, for the TS SVM model RMSE = 4.2839, MSE = 18.352, and R-square = −0.36, while for the FL SVM model RMSE = 0.75973, MSE = 0.57719, and R-square = −0.13. The considered ANFIS models include two inputs (nanoparticle type and weight percentage), and two and five membership

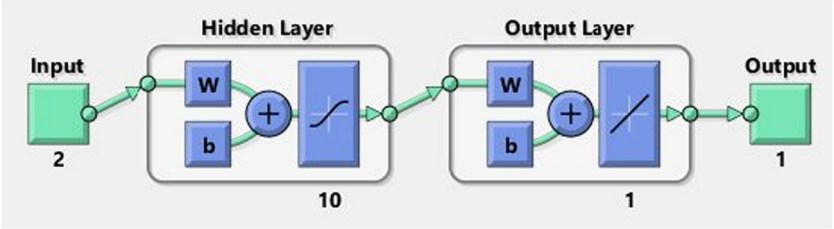

Figure 9: The ANN model structure.

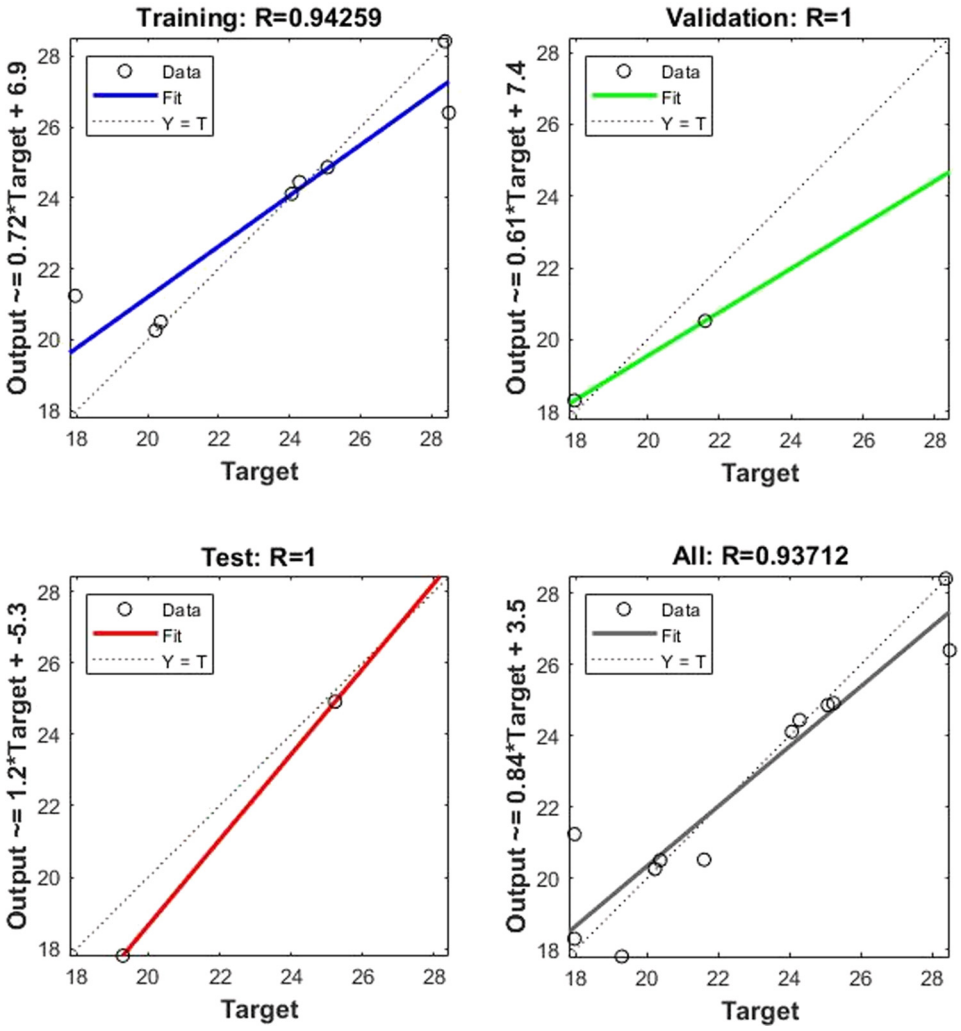

Figure 10: Regression plot of the ANN model.

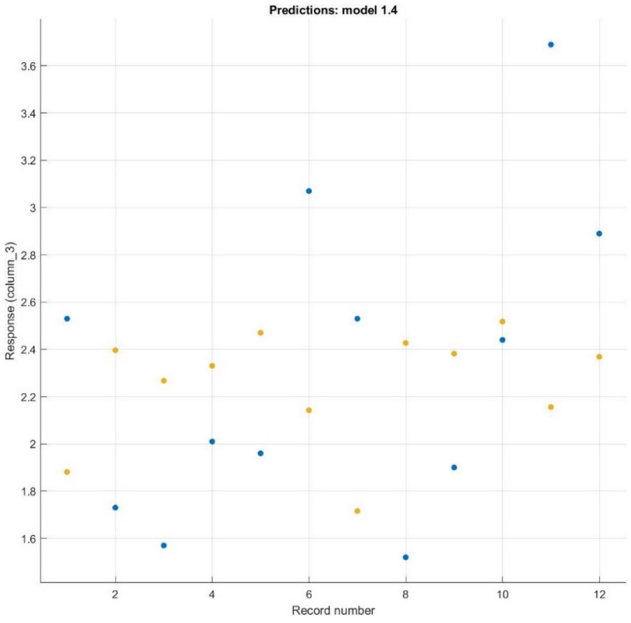

Figure 11: FL predict *versus* real SVM data.

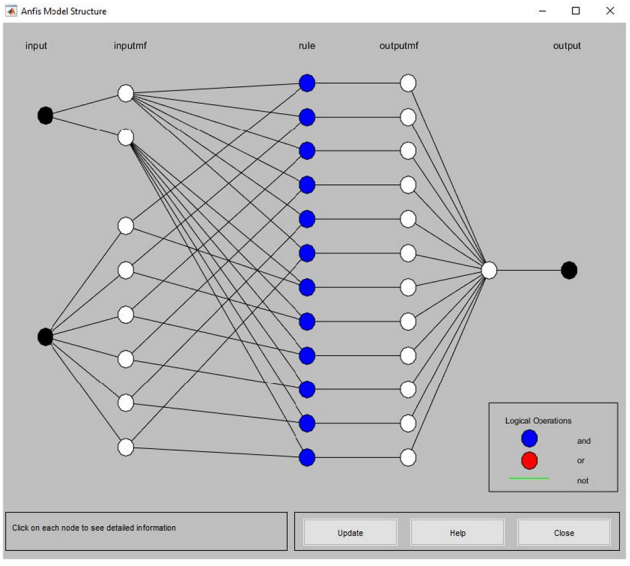

Figure 12: The ANFIS model structure.

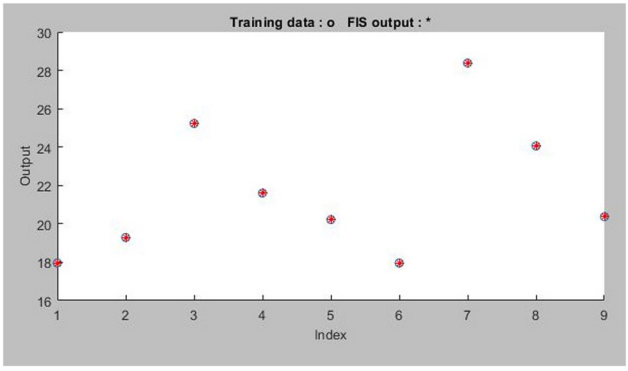

Figure 13: Plot of ANFIS for TS prediction.

functions for the first and second inputs, respectively. Figure 12 illustrates the ANFIS model structure.

ANFIS models were generated using the MATLAB Neuro-fuzzy designer tool. The models were trained using 75% of tensile and joint FL experimental results, yet the remaining 25% were for testing. The Gaussmf membership function with fixed output was used to create the FIS model. Training was completed at epoch 1, with an average testing error of 1.5265×10^{-6}. Figure 13 displays the TS ANFIS model plot, which shows the FIS output and training data.

3.3.1 ML *vs* experimental results

Table 1 lists TS results and predicted data using machine learning models of TiO_2 and GNP nanocomposites. As shown in Table 1, the predicted TS using ANN showed a drastic compliance with experimental TS results, exhibiting 3.67% prediction error, while TS values obtained from MLR, SVM, and ANFIS revealed a significant agreement with errors of 5.27, 5.37, and 6.74%, respectively. This highlights the ability of these models to be trained and

Table 1: Predicted TS values using MLR, ANN, SVM, and ANFIS

Matrix	Wt%	Experiment (MPa)	MLR (MPa)	ANN (MPa)	SVM (MPa)	ANFIS (MPa)
TiO_2	0	17.96	17.34	18.3	18.9419	17.96
TiO_2	1	19.29	19.72	17.8	19.5465	19.29
TiO_2	5	24.28	24.95	24.44	23.8802	22.3731
TiO_2	10	25.23	24.71	24.91	24.8235	25.23
TiO_2	15	21.60	21.54	20.52	22.0001	21.6
TiO_2	20	20.22	20.36	20.26	20.623	20.22
GNP	0	17.96	21.76	21.24	22.5004	17.96
GNP	1	28.49	23.92	26.4	23.8548	21.1485
GNP	5	28.38	28.27	28.41	27.2574	28.38
GNP	10	25.07	26.98	24.86	24.6729	13.2474
GNP	15	24.06	22.80	24.11	23.667	24.06
GNP	20	20.37	20.64	20.5	20.7634	20.37
Error%			5.27%	3.67%	5.37%	6.74%

Table 2: Predicted joint FL values using MLR, ANN, SVM, and ANFIS

Matrix	Wt%	Experiment (kN)	MLR (kN)	ANN (kN)	SVM (kN)	ANFIS (kN)
TiO_2	0	2.53	2.41	2.475	2.459	2.53
TiO_2	1	1.73	2.04	1.909	2.2343	1.73
TiO_2	5	1.57	1.36	1.573	1.6695	1.57
TiO_2	10	2.01	1.70	2.014	2.0799	1.3538
TiO_2	15	1.96	2.50	1.959	2.0263	1.96
TiO_2	20	3.07	2.85	2.664	3.0036	3.07
GNP	0	2.53	2.10	1.952	2.4637	2.53
GNP	1	1.52	1.95	1.937	2.2611	1.52
GNP	5	1.90	1.92	1.901	1.9664	1.5719
GNP	10	2.44	2.63	2.223	2.3993	2.44
GNP	15	3.69	3.31	3.692	3.0663	3.69
GNP	20	2.89	3.05	2.887	2.8201	0.8201
Error%			13.00%	7.21%	10.33%	10.24%

used for the prediction of the TS of nanocomposites. Moreover, GNP nanocomposite at 5 wt% exhibited the highest TS between all implemented machine learning models. The most convenient machine learning technique for the prediction of the TS of nanocomposites is ANN as it exhibited the least prediction error of 3.67%. Table 2 displays experimental overlap FL results and predicted data using machine learning techniques of TiO_2 and GNP nanocomposites.

As shown in Table 2, MLR, SVM, and ANFIS models exhibited prediction errors of 13.00, 10.33, and 10.24%, respectively. However, the overlap FL obtained from the ANN model showed the least prediction error, a value of 7.21%, which therefore can be considered the most suitable prediction approach across all the utilized models for predicting the overlap joint FL of the nanocomposites. Peak FL values were observed in the GNP nanocomposite joints at 15 wt%.

4 Conclusion

In this study, the tensile properties of TiO_2 and GNP nanocomposite were evaluated following the ASTM standard D638-14. Moreover, the considered nanocomposites were utilized as an adhesive for an overlap joint of two A5055 aluminum sheets. Then, their apparent shear strength properties were evaluated following the ASTM D1002-01 standard. Five weight percentages of different nanoparticles were considered (1, 5, 10, 15, and 20 wt%). Furthermore, for evaluating the capability of deep learning and machine learning models in predicting the mechanical characteristics of nanocomposites, the results obtained from the experiment were applied to train and test the considered models, *i.e.*, ANFIS, SVM, MLR, and ANN.

However, a maximum TS behavior was witnessed in epoxy/GNP at 1 wt%, which exhibited a value of 28.49 MPa, whereas for the overlap joints FL, the highest value recorded in this study was 3.69 kN, which was observed in epoxy with 15 wt% GNP. ANN can be considered a convenient machine learning model for the prediction of the joint failure shear load and TS of nanocomposites since it showed the least prediction error of 3.67% in predicting TS and 7.21% in the prediction of FL.

Funding information: This study was supported by the projects: VEGA 1/0172/20 and VEGA 1/0307/23 of the Scientific Grant Agency of the Ministry of Education, Science, Research and Sport of the Slovak Republic.

Author contributions: All authors have accepted responsibility for the entire content of this manuscript and approved its submission.

Conflict of interest: David Hui, who is the co-author of this article, is a current Editorial Board member of *Nanotechnology Reviews*. This fact did not affect the peer-review process. The authors declare no other conflict of interest.

References

[1] Moriche R, Prolongo SG, Sánchez M, Jiménez-Suárez A, Sayagués MJ, Ureña A. Morphological changes on graphene nanoplatelets induced during dispersion into an epoxy resin by different methods. Compos Part B. 2015;72:199–205.
[2] Khoee S, Hassani N. Adhesion strength improvement of epoxy resin reinforced with nanoelastomeric copolymer. Mater Sci Eng A. 2010;527(24–25):6562–7.
[3] Zhai LL, Ling GP, Wang YW. Effect of nano-Al2O3 on adhesion strength of epoxy adhesive and steel. Int J Adhes. 2008;28(1–2):23–8.
[4] Ekrem M, Ataberk N, Avcı A, Akdemir A. Improving electrical and mechanical properties of a conductive nano adhesive. J Adhes Sci Technol. 2017;31(7):699–712.
[5] Zhai L, Ling G, Li J, Wang Y. The effect of nanoparticles on the adhesion of epoxy adhesive. Mater Lett. 2006;60(25–26):3031–3.
[6] May M, Wang HM, Akid R. Effects of the addition of inorganic nanoparticles on the adhesive strength of a hybrid sol–gel epoxy system. Int J Adhes. 2010;30(6):505–12.
[7] Lee DG, Kim JK, Cho DH. Effects of adhesive fillers on the strength of tubular single lap adhesive joints. J Adhes Sci Technol. 1999;13(11):1343–60.
[8] Akbari V, Jouyandeh M, Paran SMR, Ganjali MR, Abdollahi H, Vahabi H, et al. Effect of surface treatment of halloysite nanotubes (HNTs) on the kinetics of epoxy resin cure with amines. Polymers. 2020;12(4):930.
[9] Saeb MR, Rastin H, Shabanian M, Ghaffari M, Bahlakeh G. Cure kinetics of epoxy/β-cyclodextrin-functionalized Fe3O4 nanocomposites: Experimental analysis, mathematical modeling, and molecular dynamics simulation. Prog Org Coat. 2017;110:172–81.
[10] Aliakbari M, Jazani OM, Sohrabian M, Jouyandeh M, Saeb MR. Multinationality epoxy adhesives on trial for future nanocomposite developments. Prog Org Coat. 2019;133:376–86.
[11] Alhijazi M, Safaei B, Zeeshan Q, Arman S, Asmael M. Prediction of elastic properties of thermoplastic composites with natural fibers. J Text Inst. 2023;114(10):1488–96.
[12] Alhijazi M, Safaei B, Zeeshan Q, Asmael M. Modeling and simulation of the elastic properties of natural fiber-reinforced thermosets. Polym Compos. 2021;42(7):3508–17.
[13] Lee C, Wei X, Kysar JW, Hone J. Measurement of the elastic properties and intrinsic strength of monolayer graphene. Science. 2008;321(5887):385–8.
[14] Balandin AA, Ghosh S, Bao W, Calizo I, Teweldebrhan D, Miao F, et al. Superior thermal conductivity of single-layer graphene. Nano Lett. 2008;8(3):902–7.
[15] Singh S, Srivastava VK, Prakash R. Influences of carbon nanofillers on mechanical performance of epoxy resin polymer. Appl Nanosci. 2015;5(3):305–13.
[16] Araby S, Li J, Shi G, Ma Z, Ma J. Graphene for flame-retarding elastomeric composite. Compos Part A. 2017;101:254–64.
[17] Araby S, Qiu A, Wang R, Zhao Z, Wang C-H, Ma J. Aerogels based on carbon nanomaterials. J Mater Sci. 2016;51(20):9157–89.

[18] Li H, Liu Y, Zhang H, Qin Z, Wang Z, Deng Y, et al. Amplitude-dependent damping characteristics of all-composite sandwich plates with a foam-filled hexagon honeycomb core. Mech Syst Signal Process. 2023;186:109845.
[19] Feng J, Safaei B, Qin Z, Chu F. Nature-inspired energy dissipation sandwich composites reinforced with high-friction graphene. Compos Sci Technol. 2023;233:109925.
[20] Pan S, Feng J, Safaei B, Qin Z, Chu F, Hui D. A comparative experimental study on damping properties of epoxy nanocomposite beams reinforced with carbon nanotubes and graphene nanoplatelets. Nanotechnol Rev. 2022;11(1):1658–69.
[21] Mustafa BS, Jamal GM, Abdullah OG. The impact of multi-walled carbon nanotubes on the thermal stability and tensile properties of epoxy resin hybrid nanocomposites. Results Phys. 2022;43:106061.
[22] Kumar A, Ghosh PK, Yadav KL, Kumar K. Thermo-mechanical and anti-corrosive properties of MWCNT/epoxy nanocomposite fabricated by innovative dispersion technique. Compos Part B. 2017;113:291–9.
[23] Safaei B, Chukwueloka EO, Gören M, Kotrasova K, Yang Z, Arman S, et al. Free vibration investigation on RVE of proposed honeycomb sandwich beam and material selection Optimization. Facta Univ Ser: Mech Eng. 2023;21:31–50.
[24] Sarkon GK, Safaei B, Kenevisi MS, Arman S, Zeeshan Q. State-of-the-art review of machine learning applications in additive manufacturing; from design to manufacturing and property control. Arch Comput Methods Eng. 2022;29(7):5663–721.
[25] Alhijazi M, Zeeshan Q, Qin Z, Safaei B, Asmael M. Finite element analysis of natural fibers composites: A review. Nanotechnol Rev. 2020;9(1):853–75.
[26] Pattnaik P, Sharma A, Choudhary M, Singh V, Agarwal P, Kukshal V. Role of machine learning in the field of Fiber reinforced polymer composites: A preliminary discussion. Mater Today. 2020;44(6):4703–8.
[27] Alhijazi M, Safaei B, Zeeshan Q, Asmael M, Harb M, Qin Z. An Experimental and metamodeling approach to tensile properties of natural fibers composites. J Polym Environ. 2022;30:4377–93.
[28] Albu A, Precup RE, Teban TA. Result and challenges of artificial neural networks used for decision-making and control in medical application. Facta Univ Ser: Mech Eng. 2019;17(3):24.
[29] Jamshidi MB, Daneshfar F, editors. A hybrid echo state network for hypercomplex pattern recognition, classification, and big data analysis. 2022 12th International Conference on Computer and Knowledge Engineering (ICCKE). Mashhad, Iran: IEEE Xplore; 2022. p. 7–12.
[30] Khalaj O, Jamshidi MB, Saebnoori E, Mašek B, Štadler C, Svoboda J. Hybrid machine learning techniques and computational mechanics: Estimating the dynamic behavior of oxide precipitation hardened steel. IEEE Access. 2021;9:156930–46.
[31] Jamshidi MB, Talla J, Peroutka Z, Roshani S, editors. Neuro-Fuzzy approaches to estimating thermal overstress behavior of IGBTs. 2021 IEEE 19th International Power Electronics and Motion Control Conference (PEMC). Gliwice, Poland: IEEE Xplore; 2021. p. 843–50.
[32] Alhijazi M, Zeeshan Q, Safaei B, Asmael M, Qin Z. Recent developments in palm fibers composites: a review. J Polym Environ. 2020;28:3029–54.
[33] Alhijazi M, Safaei B, Zeeshan Q, Asmael M, Eyvazian A, Qin Z. Recent developments in Luffa natural fiber composites. Sustainability. 2020;12(18):7683.
[34] Pati PR. Prediction and wear performance of red brick dust filled glass–epoxy composites using neural networks. Int J Plast Technol. 2019;23(2):253–60.
[35] Antil SK, Antil P, Singh S, Kumar A, Pruncu CI. Artificial neural network and response surface methodology based analysis on solid particle Erosion behavior of polymer matrix composites. Materials. 2020;13(6):1381.
[36] Jayaganthan S, Babu MS, Vasa NJ, Sarathi R, Imai T. Classification of coal deposited epoxy micro-nanocomposites by adopting machine learning techniques to LIBS analysis. J Phys Commun. 2021;5(10):105006.
[37] Rahman A, Deshpande P, Radue MS, Odegard GM, Gowtham S, Ghosh S, et al. A machine learning framework for predicting the shear strength of carbon nanotube-polymer interfaces based on molecular dynamics simulation data. Compos Sci Technol. 2021;207:108627.
[38] Nitesh, Kumar A, Saini S, Yadav KL, Ghosh PK, Rathi A. Morphology and tensile performance of MWCNT/TiO2-epoxy nanocomposite. Mater Chem Phys. 2022;277:125336.
[39] Ahmadi-Moghadam B, Taheri F. Fracture and toughening mechanisms of GNP-based nanocomposites in modes I and II fracture. Eng Fract Mech. 2014;131:329–39.
[40] Ning N, Liu W, Hu Q, Zhang L, Jiang Q, Qiu Y, et al. Impressive epoxy toughening by a structure-engineered core/shell polymer nanoparticle. Compos Sci Technol. 2020;199:108364.